

A Study on head protection performance of cyclist helmet in impact against vehicle A-pillar

Daisuke Ito¹, Koji Mizuno¹, Yong Han²

¹*Graduate School of Engineering, Nagoya University, Nagoya, Japan, 4648603*

²*School of Mechanical and Automobile Engineering, Xiamen University of Technology, 600 Ligong Road, Jimei, Xiamen, China, 361024*

Email:ito@mech.nagoya-u.ac.jp

Abstract:In this study, the helmet protection against the A-pillar was investigated from finite element (FE) simulations with models of pedestrian headform, human head and two helmets. A pedestrian headform and a human head FE models with and without the helmets was impacted against the A-pillar based on the test protocol of pedestrian protection regulation. The head injury criteria (HIC) were over 3000 despite wearing both types of helmets in A-pillar impact (35 km/h). A soft shell helmet cannot prevent skull fracture of the human model in the A-pillar impact. In the A-pillar impact simulation, the strain in the brain exceeded 10% around the vertex surface and the median plane. From the results, it is likely that the cyclist helmet was effective for the head impact on the ground during fall whereas its performance on head protection might be limited in a high velocity impact against an A-pillar.

Keywords:Finite element analysis, Bicycle helmet, Head injury

1 Introduction

According to Japanese traffic accident data for 2011 issued by the Institute for Traffic Accident Research and Data Analysis [1], the number of cyclist fatalities, serious injuries and minor injuries was 628 (13.6% of the total traffic deaths), 10,779 (22.2%) and 132,331 (16.4%), respectively.

Cyclist injuries occur in collisions with vehicles, falls, striking fixed objects, and collisions with other bicycles. The head, upper extremities, and lower extremities are the frequently injured body regions for cyclists [2]. The main sources of head injuries to cyclists and pedestrians in the vehicle are the bonnet-top, windshield, A-pillar, and roof; and the cyclist head is inclined to impact rear locations of the vehicle [3, 4].

Since cyclists frequently sustain head injuries, it is generally considered that a helmet which protects the cyclist's head is the most effective measure for injury prevention. However, it is not clear whether the cyclist helmet can prevent head injuries in A-pillar impacts because the A-pillar should be stiff enough to maintain the occupant survival space and to protect car occupants, especially for rollover and offset frontal impacts.

In this study, the helmet protection against the A-pillar was investigated from finite element (FE) simulation. First, the pedestrian headform with and without cyclist helmet was impacted against the A-pillar based on the test protocol of pedestrian protection regulation. Second, to understand the acceleration and the behavior of the headform with helmet, the contact force was examined. Finally, to investigate the injury probability of the human head during impact, the human head FE model with and without the helmet was also impacted against the A-pillar.

2 Method and Material

2.1 FE models

In order to investigate effects of helmet shell stiffness on head protection performance, two types of helmet FE models were developed (Fig. 1). Both helmet model consists of plastic shell and inner liner for energy absorption. The characteristics of the liner was shown in Fig. 2.

An FE model of the pedestrian headform was used, and the headform drop and the A-pillar impact simulations were conducted with and without the child helmet (Fig.3). In the drop simulation, the headform with or without helmet was dropped on the rigid surface from a height of 1.5 m (impact velocity was 19.5 km/h). The headform impact test was simulated against the A-pillar of the small car model (Toyota Camry) provided by the National Crash Analysis Center (NCAC). The headform impact velocity was 35 km/h and the impact angle was 65 degree. The gap between the helmet and the headform was 10 mm.

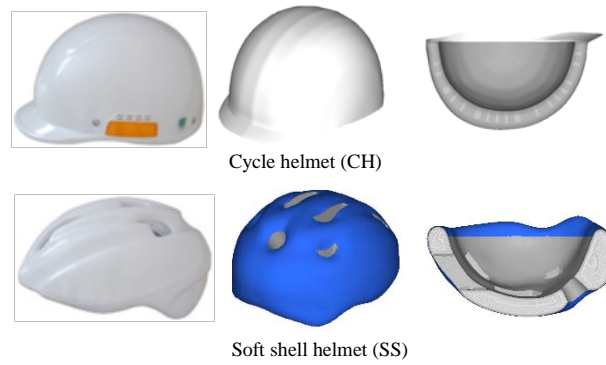


Fig. 1 Helmet FE models

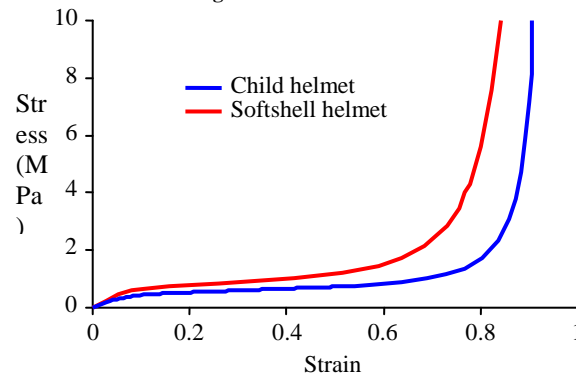


Fig. 2 Stress-strain curve of helmet liner

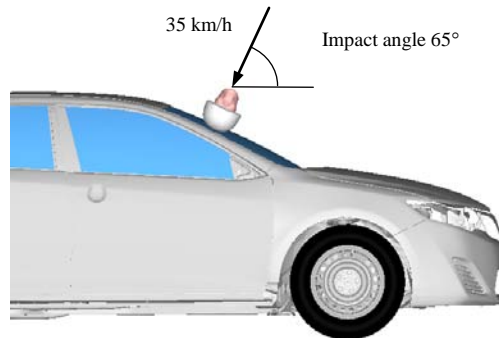


Fig. 3 Impact condition against A-pillar

In order to investigate the effectiveness of the helmet for the injury prevention, the head of a human FE model (THUMS version 4.0) was also impacted with and without the child helmet in the same impact condition of the headform. The head was dropped or impacted from its vertex.

3 Results and Discussion

3.1 Effective mass of cyclist head

Because of different impact condition of head, it should be considered whether cyclist head impact can be replaced by headform or not. In this section, effective masses m_e were calculated by using contact force between head and car and were compared actual head mass. We consider a situation that the contact force F acts on the head between time t_1 and t_2 . In $t_1 \leq t \leq t_2$, the equation of motion of the head is expressed as:

$$m_e \alpha = F \quad (1)$$

where α is acceleration of head center of gravity. In one dimensional motion, the effective mass m_e was defined by an impulse $\int_{t_1}^{t_2} F dt$ as follows:

$$m_e = \frac{\int_{t_1}^{t_2} F dt}{\int_{t_1}^{t_2} a dt} = \frac{\int_{t_1}^{t_2} F dt}{v(t_2) - v(t_1)} \quad (2)$$

When the head is hit against A-pillar as the direction of the force is not straight from travel direction, complex translational and rotational motion may be occurred, and Eq. (2) is not established in three dimensional motion. In this study, it was hypothesized the effective mass was calculated by using resultant contact force and resultant head acceleration for simplification.

In addition, we tried to obtain the effective mass from the viewpoint of mechanical energy. Integrating both sides of Eq. (1) in displacement s , we can obtain another definition of the effective mass as follows:

$$m_e = \frac{\int_{s_1}^{s_2} F \cdot ds}{\int_{s_1}^{s_2} a \cdot ds} = \frac{\int_{t_1}^{t_2} F \cdot v dt}{\int_{t_1}^{t_2} a \cdot v dt} \quad (3)$$

In this equation, the relation $ds = v dt$ was used.

In order to evaluate the effective mass in car-to-cyclist collision, a FE simulation was performed with a human FE model, a bicycle model and a car model. The THUMS occupant FE model (ver. 3) which is 175 cm in height and weighs 77 kg was used as the cyclist. The human model was set to be in the posture with the right leg forward and the left leg backward and was placed on the bicycle model. Both left and right arms were positioned on the handlebar. The initial condition of simulation and comparison of position with a pedestrian are shown in Fig. 4. The cyclist with the bicycle was placed in front of the right A-pillar of the car model and was facing laterally. In this simulation, the bicycle velocity was set at 0 km/h and the impact velocity of the car was set at 40 km/h. Simulation of a car-to-pedestrian collision at an impact speed of 40 km/h was also performed with the same car model (Fig.4 (b)). In these simulations, the heights of the pelvis were at the same level and only the postures of the lower extremities were different.

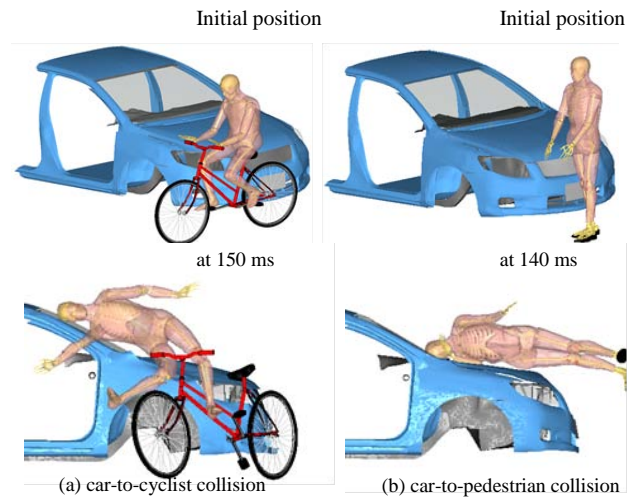


Fig. 4 Initial condition and kinematics of cyclist and pedestrian in car collision

Figure 5 shows calculation of the effective mass derived by Eqs. (2) and (3). The time t_1 and t_2 was defined as the time when the contact force reached 10% of the maximum value. The effective mass of the cyclist was estimated as 3.6 kg (83% of the actual head mass). Consequently, it was considered that cyclist head impact could be replaced with headform impact test.

While the effective mass was larger than actual head mass (4.2 kg) in the pedestrian impact, it was smaller in the cyclist impact. This is because neck axial force of cyclist was larger than that of pedestrian due to different whole body kinematics. Though the pedestrian wrapped around frontal shape of the car in impact, the cyclist dived headfirst into the A-pillar and the body below the neck pushed the head into the A-pillar (Fig.4).

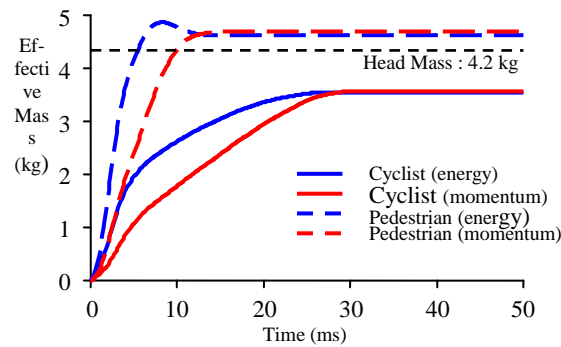


Fig. 5 Effective masses of head of cyclist and pedestrian in car collision

3.2 Headform FE model analysis

The headform impact simulation was conducted for the drop test and the A-pillar impact. Figure 6 shows the helmet deformation. The helmet liner deformed flat against the floor in the drop test simulation whereas it deformed locally and bottomed out in the A-pillar impact though the A-pillar deformation was small. Figure 7 shows the acceleration of the headform in the drop test. The headform deceleration was decreased substantially by the helmet energy absorption. Figure 7 shows the headform acceleration in the A-pillar impact test. The liner of the helmet deformed and bottomed out locally by the A-pillar at 5 ms. The A-pillar also deformed from 2 to 7 ms though the A-pillar deformation was small. The time duration was longer in the A-pillar impact than that in the drop test. The reduction of the headform acceleration by the helmet was not so large in the A-pillar impact as compared to the drop test simulation (Fig. 7 and 8).

Table 1 presents the HIC and the maximum acceleration of the headform in the drop and A-pillar impact simulations. In the drop simulation, the HIC was reduced substantially from 11142 to 1432 and 1072 by the helmet. On the other hand, the HIC was not reduced so much by the helmet in the A-pillar impact. This is because the helmet liner bottomed out immediately after the contact and the HIC value depended on the high acceleration level from 3 to 5 ms where the A-pillar deformed with constant collapse force. Though the helmet liner could absorb the impact energy (19.5 km/h) efficiently in the drop test simulation, the impact energy was too large to be absorbed by the liner in the A-pillar impact (35 km/h).

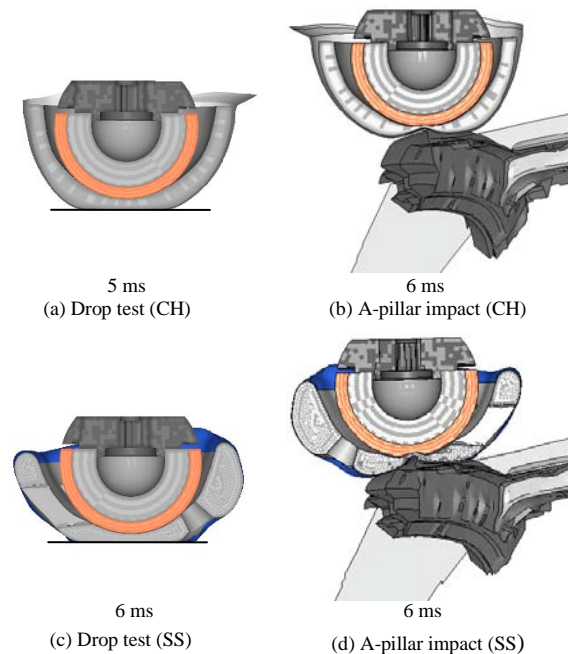


Fig. 6 Deformation of helmet liner in car collision

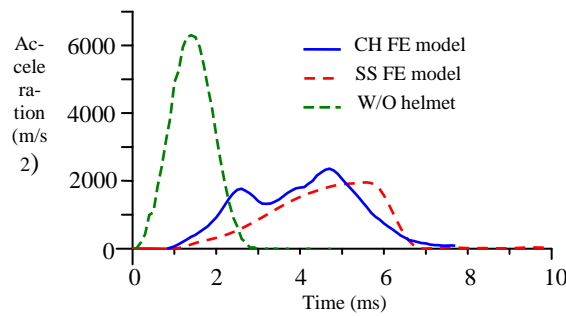


Fig. 7 Acceleration of headform in drop simulation

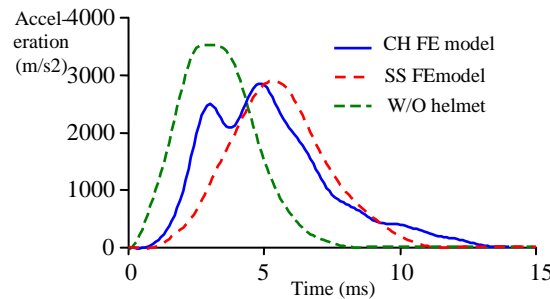


Fig. 8 Acceleration of headform in A-pillar impact simulation

Table 1 HIC and maximum acceleration of headform in drop simulation and impact simulation against A-pillar

		Without helmet	Child helmet	Soft shell helmet
Drop (1.5m)	HIC	11142	1427	1072
	Max acc.	6860	2360	1960
A-pillar impact	HIC	5210	3624	3318
	Max acc.	3606	2849	2850

3.3 Mechanism of head acceleration of the headform with helmet

To understand the acceleration and the behavior of the headform with helmet, the contact force was examined. Designating the mass of the headform as m_{head} and headform with a helmet as m_{helmet} , the contact force between the helmet and the headform as $F_{\text{helmet/head}}$, and the contact force between the helmet and the external object (object: floor or A-pillar) as $F_{\text{helmet/object}}$, the motion of equation of the helmet and the headform is expressed as:

$$m_{\text{helmet}} a_{\text{helmet}} = F_{\text{helmet/object}} - F_{\text{head/helmet}} \quad (4)$$

$$m_{\text{head}} a_{\text{head}} = F_{\text{head/helmet}} \quad (5)$$

From Eqs. (4) and (5), the head acceleration can be calculated as:

$$m_{\text{head}} a_{\text{head}} = F_{\text{helmet/object}} + m_{\text{helmet}} a_{\text{helmet}} \quad (6)$$

Accordingly, the headform acceleration depends on the helmet force and the helmet inertia force.

Figure 9 shows the contact force and the inertial force in the drop and the A-pillar impact simulations. From Fig. 9(a)(c), the helmet inertial force ($m_{\text{head}} a_{\text{head}}$) and the force difference ($F_{\text{helmet/object}} - F_{\text{head/helmet}}$) were comparable, which indicates that Eq.(4) is valid. Initially, the helmet made contact with the object, rebounded in the upper direction and impacted the dropping headform. This led to the helmet acceleration (a_{helmet}) oscillation: the force was exerted on the helmet from the impact object (floor or A-pillar) and the headform. As a result, a first peak was generated in the $F_{\text{head/helmet}}$ (Fig.9 (c)(d)). This peak could be observed in the experiments: in the headform impact tests of child helmet, the initial peak of the acceleration was high probably because of the heavy mass of the helmet shell. After, the first peak of the headform acceleration, the dropping headform pushed the helmet downward and made contact against the floor together, which led to the maximum headform deceleration. Consequently, the acceleration of the helmet was influenced by the helmet liner deformation characteristics as well as the helmet inertia force.

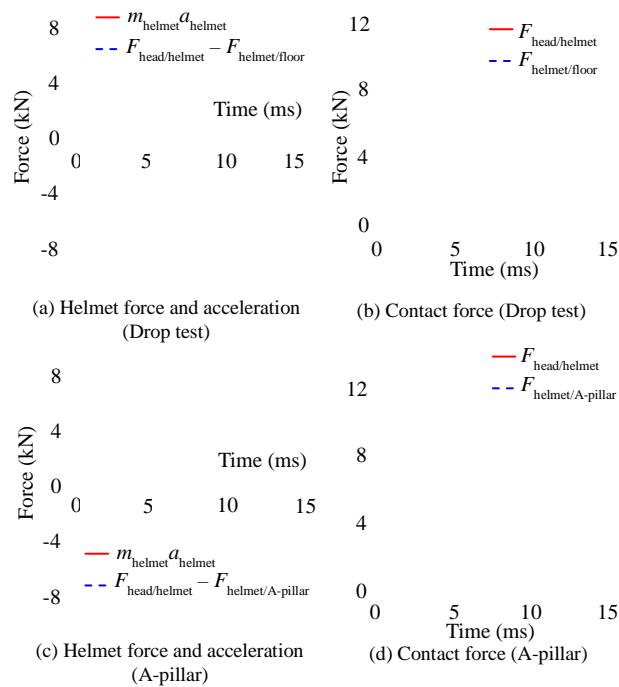


Fig. 9 Force applied on the helmet in drop test and A-pillar impact simulation

3.4 Human head FE model analysis

The protection provided by the helmet in the drop and the A-pillar impact was also examined using the human FE model. Figure 10 shows the skull deformation with and without the child helmet, and in the drop test simulation (19.5 km/h), the vault fracture occurred for the head without wearing the helmet. With wearing the helmet, the impact force was attenuated and distributed by the helmet liner, and the stresses were distributed on the vault. The strain of the brain was less than the injury threshold (10%).

In the impact against the A-pillar (35 km/h), though the helmet deformed locally due to contact with the A-pillar, the stresses on the skull also were distributed by the helmet liner, and the vault fracture did not occur when the CH helmet was worn (Table 2). However, the skull fracture occurred in the SS helmet case. This is because stiffness of outer shell of the SS helmet (thickness: 0.3 mm) is weaker than that of CH helmet (3.5 mm). Therefore, the dispersion effect of impact force is lower and the helmet liner bottomed out in high speed impact and as a result, high stress on the skull was generated despite wearing the helmet.

Figure 11 shows the maximum principal strain of the brain in A-pillar impact. As shown in Fig. 11, the brain strain was more than 10% around the vertex surface and the median plane because of contact with the falx cerebri though it was less than the injury threshold level of 10% for most of regions in the brain.

In general, it is thought that widespread high strain in brain is observed when head is subjected to high rotational acceleration and subsequently resulted in diffuse axonal injury. However, in this simulation, only small rotation around mediolateral axis and low strain in brain were observed because the head was impacted straight from its vertex. It may be possible that, if head was subjected to large rotational acceleration due to various whole body kinematics and head impact conditions (impact velocity, angle and location), brain injury risk becomes high in A-pillar impact. Further research should include evaluation of effects of rotational motion of head on brain damage and reduction of the rotational motion by using helmet.

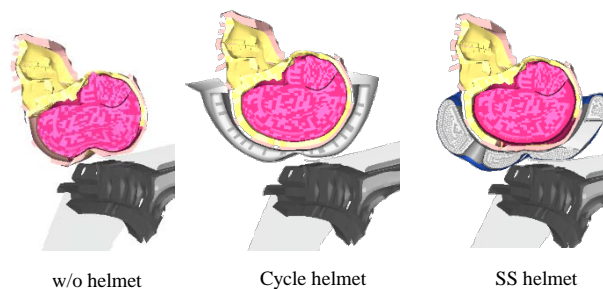


Fig. 10 Skull and brain deformation in A-pillar impact

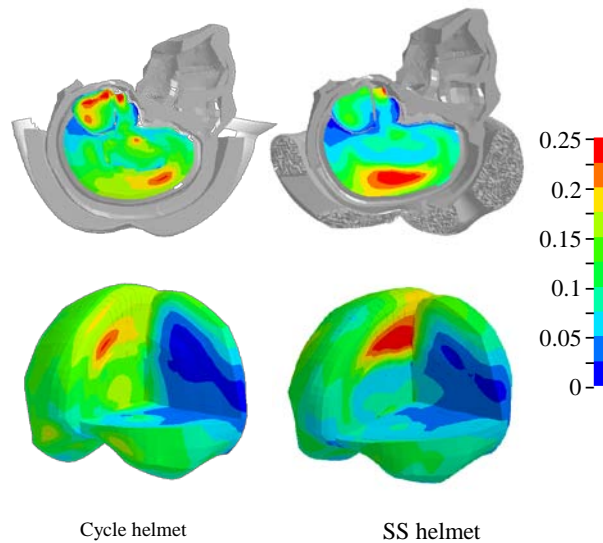


Fig. 11 Distribution of maximum principal strain in brain in A-pillar impact

Table 2 HIC and maximum acceleration of with and without helmet in FE simulation

	Headform impactor		Human model	
	Cycle helmet	SS helmet	Cycle helmet	SS helmet
Drop (1.5 m)	HIC 1427 56 %	HIC 1072 18 %	None	None
A-pillar	HIC 3624 99 %	HIC 3318 99 %	None	Fracture

4Conclusions

In this study, the effectiveness of the cyclist helmet was examined using the pedestrian headform in the drop test simulation and impact test simulation against an A-pillar with a headform and a human head model to understand the helmet energy absorbing behavior. The conclusions are as follows:

- Whereas the helmet liner could absorb the energy in the drop test at the height of 1.5 m (19.5 km/h), the impact energy was too high for the liner in the A-pillar impact (35 km/h). Therefore, it is likely that the cyclist helmet was effective for the head impact on the ground during fall whereas its performance might be limited in a high velocity impact against an A-pillar.
- Using a human FE model, the skull fracture did not occur both in the drop test (19.5 km/h) and in the A-pillar impact (35 km/h) simulations when the CH helmet was worn. However, the skull fracture occurred in the SS helmet case. In addition, in the A-pillar impact simulation, the strain in the brain exceeded 10% around the vertex surface and the median plane.

Acknowledgement

This research study was conducted under the grant of the High-End Foreign Experts Recruitment program of China (GDT20143600027). We wish to thank Mr. Keiji Oidain performing the large number of simulations.

References

- [1] ITARDA, Traffic accident statistics, 2011 (in Japanese).
- [2] Otte, D., Jansch, M., Haasper, C., Injury protection and accident causation parameters for vulnerable road users based on German in-depth accident study GIDAS, Accident Analysis and Prevention, 2012 44(1) 149-153.
- [3] Maki, T., Kajzer, J., Mizuno, K., Sekine, Y., Comparative analysis of vehicle-bicyclist and vehicle-pedestrian accidents in Japan, Accident Analysis and Prevention, 2003 35(6) 927-940.
- [4] Otte, D., Head impact conditions and injury pattern in car crashes against pedestrians versus bicyclists in German in-depth accident study GIDAS, International Crashworthiness Conference, Washington, D.C., 2010